7

Load Transfer Along the Bone-Implant Interface and Its Effects on Bone Maintenance

Samira Faegh, Hsuan-Yu Chou and Sinan Müftü
Northeastern University, Department of Mechanical Engineering
Boston, Massachusetts
USA

1. Introduction

The long term success of dental implant treatment relies on the proper stability of the implant within the host bone. This condition is achieved through osseointegration, which is characterized as a direct functional and structural connection between ingrown bone tissue and implant surface (Brånemark et al., 1977; Simmons et al., 2001). Osseointegration begins with rapid growth of random and unorganized woven bone around the implant, while a biomechanically favorable environment at the bone-implant interface develops (Leucht et al., 2007; Schenk & Buser, 1998). This initial bony structure is maintained by bone remodeling and bone adaptation, where woven bone is slowly replaced by more organized lamellar bone. Adaptation of bone morphology in response to functional loads continues throughout life (Schenk & Buser, 1998).

The load transfer from the implant to the host bone depends on the amount of bone surrounding the implant and in turn affects the success of treatment, by the load transfer from the implant to the host bone. X-ray imaging, computerized tomography (CT), and histomorphometric evaluation of the extracted implants provide insightful information about the quality and quantity of peri-implant bone. However, systematic evaluation of the mechanism of load transfer and its effect on peri-implant bone remodeling is difficult via aforementioned techniques, due to the cost and effort involved and due to the associated ethical concerns. Reliable computational models can be useful to predict the long term outcome of a dental implant treatment, and thus help with the decisions related to implant treatments and design. In this paper, a state of the art review of the computational models used in evaluating the biomechanics of dental implant systems is provided. The literature shows that load transfer along the bone-implant interface is not well understood, despite the fact that the bone loading starts along this interface.

Recently a systematic investigation of the effects of various parameters related to a dental implant's contour including the implant's diameter, body-length, collar length and slope, and the morphology of the external threads was carried out by Faegh and Müftü (2010). The variation of normal and shear stresses along the bone dental-implant interface was investigated. Here, in order to generalize the bone morphology an elliptical contour is used. The results are compared to a similar recent study in which the bone contour was drawn from a CT image of the incisor region (Faegh & Müftü, 2010).

1.1 Factors that influence the load transfer from implant systems to bone

Load transfer from the implant to the bone has been identified as one of the critical factors that determine the long term success of dental implant treatment (Duyck et al., 1997; Morris et al. 2001). Load transfer is influenced by several factors including: (i) the loading type, (ii) the length and diameter of implant, (iii) the implant shape, (iv) the structure of the implant surface, and (v) the bone quality (Duyck et al., 1997). A simple, analytical solution of the stress/strain distribution in the bone for an implant treatment scenario is not feasible, due to the complex geometry of the bone and the dental implant system. Photoelesticity (Farah et al., 1979; Kinni et al., 1987; Munir et al., 1975) and finite element analyses have been increasingly used in this field (Cook et al., 1980, 1982a, 1982b; Geng et al., 2001;) to analyze the stress distribution for different root form implant designs (Bozkaya et al., 2004; Hansson, 1999; Holmgren et al, 1998; Rieger, 1988; Rieger et al., 1989a, 1989b, 1990a, 1990b; Siegele & Soletz, 1989) prosthesis designs (Papavasiliou, et al. 1996a, 1996b; Stegaroiu et al. 1998a, 1998b) and for various clinical scenarios (Akça & İplikçioğlu, 2001; Canay et al., 1996; Gross & Laufer, 1997; İplikçioğlu & Akça, 2002; Meijer et al., 1994; Pierrisnard et al., 2002; Tuncelli et al., 1997; van Oosterwyck et al, 2002).

Over the years, numerous implant designs and clinical protocols emerged, sometimes dictated by market demands (Brunski, 1999). Currently, there are more than 50 implant designs available in the market. Research and development in the dental implant field led to significant progress in areas and applications that were previously limited. For example, implants can be successfully inserted in areas of reduced bone height and high functional load, such as the posterior segments of mandible and the maxilla. Moreover, advances in our understanding of the mechanobiology led to design of implant systems that can function immediately after insertion (Balshi & Wolfinger, 1997a; Brånemark et al., 1999; Brunski, 1999; Chow et al., 2001; Ericsson et al., 2000; Jaffin et al., 2000; Salama et al., 1995; Tarnow et al., 1997).

1.1.1 Bone-implant connection

One of the main drivers for different implant designs is to improve bone-to-implant connection. Osseointegeration, first described by Brånemark et al. (1977, 1985), defines the direct connection of bone and implant. Osseointegration involves chemical bonding of the tissue to the implant, as well as micro- and macro-level mechanical interlocking of the bone with the features on the implant surface. Chemical and morphological modifications of the outside surface of the implant material have been shown to enhance connection strength and reduce the healing time. To this end, bioactive ceramics such as hydroxyapatite have been used as coatings on the implant surface. Such coatings have been shown to improve bone-implant fixation through chemical bonding between the implant and the surrounding tissues. Surface morphology of implants can be modified in macro-level through the designs of external threads, undercuts and layers of wires, and in micro-level by increasing surface roughness.

Shape and chemistry of the bone-implant interface influence the stress distribution in the bone for different implant designs (Bidez et al., 1988; Hipp et al., 1985). Siegele and Soltesz (1989) modeled different bone-to-implant connection types by using frictional contact. Their work showed that high levels of bone stresses occur in the apex region of the implant if perfect osseointegration is assumed, whereas the high stress region occurs in the alveolar crest for frictional sliding contact condition. Similar results for the perfectly bonded interface have been reported by Weinstein et al. (1976).

Strength of bone fixation depends in part on the mechanical properties of the bone surrounding the implant. One common metric of bone quality is the bone density levels (Lekholm and Zarb, 1985). Whether the implant is surrounded by cortical bone or trabecular bone makes a significant difference in interfacial stresses (Borchers & Reichart, 1983; Lavernia et al., 1982). Lavernia et al. (1981) reported significant change in stress magnitude when bone properties are switched between trabecular and cortical. Kitoh et al. (1978) and Bozkaya et al. (2004) showed that the occlusal force applied to the implant is supported primarily by the cortical bone.

1.1.2 Implant-contour

The long term outcome of the implant treatment is influenced by the loading experienced by the bone, in several different respects. In general, excessive micro-motion of the bone-implant interface should be avoided, while providing adequate stimulation to promote healing and remodeling response (Brunski, 1999). The shape of the implant contour, and its local features have a considerable influence on bone healing and maintenance. Siegele and Soltesz (1989) compared the load transfer characteristics of five different implant shapes. Considered contours were cylindrical, conical, stepped, internally hollow cylindrical and externally threaded. They showed that under vertical load, lower stresses are induced in the bone with smoother implant shapes such as cylindrical, rather than implants with small radii of curvature such as the conical shape and implants with geometric discontinuities such as stepped implant contours. Under lateral loading, large stresses were observed in the apex area of the hollow cylindrical implant, and below the uppermost thread of the externally threaded implants. Holmgren et al. (1998) reported that the stepped implant design levels out the stress distribution better than a cylindrical design. Rieger et al. (1989a, 1990a, 1990b) investigated the effect of implant geometry and the elastic modulus of the implant materials on the stress distribution for different implant designs. A tapered design made of a material with high elastic modulus was concluded to be the most suitable design in their study. Weinstein et al. (1976) investigated a porous rooted dental implant and concluded that high bone-level stresses are induced near the apex of the implant in a model with continuously bonded interface. In their comparative evaluation of five commercially available implant systems, Bozkaya et al. (2004) showed that implant systems with internally sloping crestal modules are better at reducing the bone overload in the cortical bone, whereas systems with widening crestal-modules cause bone overload in compression. Kong et al. (2008) suggested that neck taper (collar slope) ranging from 64° to 70°and end (apex) fillet exceeding 0.8 mm result in the optimal stability of implant.

Siegele and Soltesz (1989) reported a high failure rate in the hollow cylindrical implants due to low primary stability. Moreover, the conical or shoulder-type implants distributed high stress level at the bone interface. Rounding off the corners of the implant was found to have a significant effect on reducing the stress (Siegele & Soltesz, 1989). Faegh and Müftü (2010) showed that cylindrical implants with no external threads induce low stresses along the bone-implant interface in the trabecular region, and indicated that this might lead to inadequate bone stimulation. Cylindrical implants are no longer recommended due to problems with osseointegration and high failure rates (Schenk & Buser, 1998).

Vaillancourt et al. (1995) investigated the possible causes of bone loss in the crestal bone surrounding both porous-coated implant and non-porous-coated regions of a partially coated implant designs. They reported that lower stress level was transferred to the crestal bone region in the case of partially-porous implant, where crestal bone loss was mostly observed. They attributed this to disuse atrophy. A sufficient stress level of 1.6 MPa was reported to avoid bone loss resulting from disuse atrophy by histological studies.

1.1.2.1 Externally threaded implants

There are several advantages associated with externally threaded implants. Threads improve primary implant stability during the implant insertion (Misch, 1999b) and thus reduce micro-motion during the post insertion healing period until the stable osseointegration is established. This characteristic is of more importance in the regions of low bone density and in the submerged implant placement modality (Frandsen et al, 1984). In addition, applied (mastication) forces are diverted in normal and tangential directions to the faces of the thread and amplified in certain thread locations. This is beneficial in providing adequate loading for long term bone maintenance (Faegh & Müftü, 2010). Finally, bone growth between the threads provides the macro-level interlocking. There are different types of externally threaded implants available in the market, which vary in thread pitch, shape and depth. Since the morphology of screw threads plays an important role in the load transfer from dental implant to the surrounding bone (Frandsen et al, 1984), usage of different thread configurations for different bone qualities have been suggested (Misch, 1999a, 1999b; Misch et al., 1998, 1999, 2001).

In a finite element study carried out by Moser and Nentwig (1989), it was observed that using screw threads with an apically increasing screw thread depth reduces tension in the cervical area when implant was apically loaded. Similarly, Huang et al. (2010) suggested that external threads reduce the stress and sliding at the interface. Chun et al. (2002) reported that maximum effective stress in the cortical bone is higher in the plateau design as compared to the triangular or square thread designs. In another study carried out by Patra et al. (1998), tapered thread design implants were found to distribute higher stress levels in bone as compared to the parallel profile thread. Use of external threads on the implant body with some micro-scale roughness was reported to enhance osseointegration (Skalak, 1988). It was observed that inclined faces of threads allow for normal stress to be carried perpendicular to the interface. Transmission of shear stress can benefit from microasperities on the interface which work along each of the faces of a screw in a similar way that the screw threads work (Skalak, 1988). Faegh & Müftü (2010) carried out a systematic analysis of various implant designs with and without external threads. They showed that threads increase the interfacial stresses locally and could help in stimulating bone remodeling.

1.1.2.2 Implant diameter

Wider diameter implants provide increased implant-bone contact area, enable the engagement of the implant to the buccal and lingual (BL) faces of the bone, and have the ability to occupy the tooth socket especially in the posterior regions. These inherent characteristics of wide diameter implants significantly improve initial implant stability, which leads to the increase in likelihood of osseointegration (Langer et al., 1993; Renouard et al., 1999; Trauhlar et al., 1997). Wide diameter implants also provide higher mechanical strength to avoid implant fractures (Jarvis, 1996). Wide and short implants provide the advantage of avoiding sinus elevations and extensive bone augmentation procedures in regions of limited bone height due to the existence of alveolar nerve in the mandible and maxillary sinus in the maxilla, and potentially prevent the costs associated with bone grafting procedures (Blatz et al., 1998; Graves et al., 1994; Jarvis, 1996; Langer et al., 1993). Overall advantages of wide diameter implants include improved prosthetic stability,

reduced screw loosening, reduced incidents of implant fracture, and more optimal force distribution in qualitatively and quantitatively poor bone (Mahon et al., 2000).
Griffin et al. (2004) conducted a clinical study investigating the application of 6×8 mm hydroxyapatite coated screw retained implants in the mandibular and maxillary molar regions and reported a 100% success rate. They observed that significant stress concentration distributed to the crestal cortical bone, at the level of the first few threads and concluded that the use of long implants to provide a larger surface area for stress distribution is not necessary. Instead larger surface area provided by wide diameter implants was deemed to be better. On the other hand in a retrospective study conducted by Aparicio & Orozco (1998) the success rates of 5 mm- and 3.75 mm-diameter implants were reported to be similar in the maxilla, while higher success rate was observed for 3.75 implants in the mandible. They attributed the high failure rate in the mandible to the overheating during surgical bone drilling, excessive tightening force during implant placement, and variations of the remodeling response of the cortical bone caused by extensive drilling.
Geramy & Morgano (2004) conducted a finite element analysis comparing displacement of a standard diameter and a wide diameter implant under an occlusal load applied at the distobuccal cusp tip, and concluded that increasing the diameter of the implant will reduce both mesiodistal and buccolingual displacement of the implant system by approximately 50%. Davarpanah et al. (2001) evaluated the resistance to fracture and depth of insertion of wide diameter implants versus standard diameter implants. They found that wider diameter implants demonstrate more resistance to fracture than standard implants, which is attributed to increased surface area. Jarvis (1997) compared the 3.7 mm and 4.7 mm diameter implants and concluded that wider diameter implants decrease the induced load on the abutment screw which results in reducing implant fracture, and also the vibration of the implant that leads to loosening. Mahon et al. (2000) evaluated the stress distribution using implants with diameters 3.25, 3.75, 4, 5, and 6 mm under a load of 176 N applied 5 mm off axis. They observed that the mean stress level was highest for the 3.25 mm-diameter implant, and lowest for the 6 mm-diameter implant. High stress levels were located at the necks of the 3.25 mm implant which was consistent with the high deformation which occurred in these regions. They observed that stress level for 3.75, 4, and 5 mm diameter implants did not demonstrate large differences, however, 6 mm diameter implants showed the most reduction in the stress level. Due to this observation, they concluded that the implant diameter must be greater than a certain value in order to reduce the stress significantly. Li et al. (2011) suggested that implant with diameter greater than 4.0 mm and length longer than 12.0 mm is the optimal selection to treat tooth loss at the at locations with poor bone quality (ie. posterior mandible). Huang and Tsai (2003) reported that increasing the implant diameter and consequently the bone-implant contact area reduces stress concentration and results in improving implant stability. Chou et al. (2010) showed that the insertion depth and implant diameter affect the biomechanical response of bone, particularly between the plateaus of an implant. They indicated that the strain distribution can be optimized for long-term bone maintenance by adjusting the insertion depth for different levels of bone quality in the alveolar ridge.

1.1.2.3 Multiple implants

Using two narrow implants to support prosthesis in posterior regions has been an alternative solution to the wide diameter implant (Langer et al., 1993; Lazzara, 1994; Moscovitch, 2001). Balshi & Wolfinger, (1997b) stated that two implants maintain a more natural replacement of the missing tooth in position and direction, and allow for the preservation of the crestal bone. Mahon et al. (2000) and Trauhlar et al., (1997) stated that use of two implants also provides a more appropriate support against buccolingual and mesiodistal bending, decreases the rotating forces around the implant axis, offers greater surface area and better biomechanical properties, and maintains prosthesis retrievability. However, there are some restrictions on using two narrow implants in the posterior regions. One of these is the cone space availability buccolingually and mesiodistally (Graves et al., 1994).

Geramy et al. (2004) compared the use of a wide diameter implant with the use of two implants and reported that use of two implants to support the restoration reduces the buccolingual displacement to the same level as the 5 mm-diameter implant. Stress distribution for both wide diameter implants and two implant design systems were compared by Balshi and Wolfinger (1997b), who concluded that the percentage of stress reduction was almost identical for both designs. In a study conducted by Bahat and Handelsman (1996), the failure rate of the 5 mm-diameter implants was 2.3% compared to the 1.6% failure rate of the double implants. They suggested using double implants to support restorations rather than a single implant in the molar regions, even though there were some disadvantages associated with using double implants, such as greater bone loss and higher prosthesis mobility. On the other hand, Sato et al. (2000) concluded that using double implants in molar areas does not always reduce loads on the implants however eliminates torque. They observed higher stress levels near the marginal ridge of the superstructure compared to stress field on the wide diameter implants.

1.2 Bone remodeling (cell interactions)

Unlike the bone growth or bone modeling which mostly occurs in the early age of skeletal development, bone remodeling is a process of continuous cellular activities to replace aged, injured and dead bone. Bone remodeling is a process that is composed of two consecutive, and interrelated physiological activities, namely bone resorption and bone formation. Remodeling is carried out by basic multicellular/bone metabolic units (BMUs). Normally, osteoclasts, which are responsible for resorption, are inhibited by osteoprotegerin (OPG), which is a protein secreted by osteoblasts as inhibitory signal (Carda et al., 2005). The osteoclastic resorption is signaled by the circulating parathyroid hormone and locally secreted receptor activator nuclear kappa-b ligand (RANKL), which binds to RANK receptors on the membrane of osteoclasts (Marx, 2007). In addition to OPG, osteoblasts also secrete RANKL so that the activation of osteoclasts and the amount of resorption are regulated.

When remodeling is activated, osteoclasts are first recruited to bone surface and start to excavate the bone by releasing hydrochloric acid to dissolve the inorganic matrix, and collagenases to break down the organic matrix (Marx, 2007). A tunnel with approximately 200 μm in diameter and 300 μm long is dug at the rate of 40 μm/day (Martin et al., 1998). Following the resorption, there is reversal phase before the initiation of formation. A cylindrical space in the tunnel can be observed and the length of this region varies with the lag between the resorption and formation.

During bone resorption, some bone morphogenic proteins and insulin-like growth factors are released as active cytokines (growth and differentiation factors), which induce the differentiation of stem cells into osteoblasts (Marx, 2007). Bone formation is conducted by the osteoblasts, which refill the space with unmineralized bone matrix, osteoid, at a rate of about 1-2 μm/day (Martin et al., 1998). As the osteoblastic activity continues, a tunnel with 40-50 μm in diameter called Haversian canal is left for the transportation of the nutrients to bone cells. Finally, the bone matrix deposited by osteoblasts is mineralized and turns into Haversian system, osteon. Osteoclastic activity restores to quiescent condition under the influence of osteoblasts, and bone is maintained until the aging or diseased bone triggers the secretion of RANKL by osteoblasts (Marx, 2007).

1.2.1 Theoretical models of bone remodeling

Wolff (1892, 1986) observed that internal structure and density of bone depends on the load that it carries. It is generally well established that this functional adaptation is the result of the BMU activity as described above, which is triggered by some mechanical stimulus that BMUs can sense. Several theoretical models were formulated in order to quantitatively describe the functional adaptation of the bone (Hart, 2001). These models assume that a mechanical control signal (remodeling stimulus) governs the bone density regulation, and the BMU has the capability to respond to the changes in this signal. A biomechanical equilibrium or homeostatic state is assumed, so that bone remodeling is only triggered when the control signal deviates from this equilibrium state. Remodeling activity continues until the biomechanical equilibrium is restored and new bone morphology is established. This approach neglects the effects of hormonal, genetic and metabolic factors on bone regulation.

1.2.1.1 Mechanostat hypothesis

Frost proposed the mechanostat, which is a non-linear switch, to explain his experimental observations of bone remodeling (Frost, 1987, 2003). He used strain as the mechanical control signal, and divided the remodeling response to four different regimes. Each regime, which he called "window," is separated by threshold strains levels. These minimum strain levels were called minimum effective strain (MES). The disuse window (DW) is the lowest strain regime. If the bone is exposed to strain levels in DW for a prolonged duration, Frost's hypothesis states that decrease in bone mass will occur. Adapted window (AW) is where bone strength is naturally accepted to sustain the strain level caused by normal daily activities. Increased strain level to the mild overload window (MOW) promotes increase of bone mass. However, further increase of strain will lead to the pathologic overload window (POW) and generate internal micro damage that cannot be repaired by normal cell activities. The following relation gives a compact representation of the mechanostat hypothesis in terms of the MES:

$$\text{Bone tissue response} = \begin{cases} \text{DW}: & \text{reduced bone mass}; & \text{strain} < \text{MESr} \\ \text{AW}: & \text{constant bone mass}; & \text{MESr} < \text{strain} < \text{MESm} \\ \text{MOW}: & \text{increased bone mass}; & \text{MESm} < \text{strain} < \text{MESp} \\ \text{POW}: & \text{bone damage}; & \text{MESp} < \text{strain} \end{cases} \quad (1)$$

where MESr is the threshold of disuse remodeling; MESm is the modeling threshold; and MESp is the pathologic threshold. Note that what type of strain measure to be used in this theory was not precisely stated.

1.2.1.2 Bone remodeling base on strain energy density

Huiskes et al. (1987) suggested strain energy density U as the remodeling stimulus, and they proposed that the change of bone's elastic modulus (E) can be described as,

$$\frac{dE}{dt} = \begin{cases} C_e\left(U - (1+s)U_n\right); & U > (1+s)U_n \\ 0; & (1-s)U_n \le U \le (1+s)U_n \\ C_e\left(U - (1-s)U_n\right); & U < (1-s)U_n \end{cases} \quad (2)$$

where C_e is a remodeling constant, U is the strain energy density of bone due to loading, U_n is the homeostatic equilibrium strain energy density, and s is the fraction of U_n indicating the width of lazy zone, where no net change of elastic modulus takes place. The lazy zone and the AW appear to describe the same phenomena where the bone's elastic modulus does not depend on the remodeling stimulus, in other words it is in equilibrium.

Weinans et al. (1992) proposed a remodeling stimulus (S) that depends on, not only the strain energy density, but, but also on the bone density ρ , and on different types of loadings as follows,

$$S = \frac{1}{n}\sum_{i=1}^{n}\left(\frac{U_i}{\rho}\right) \tag{3}$$

where n is the total number of load types (i) that induce strain energy density (U_i). The density change was expresses as,

$$\frac{d\rho}{dt} = \begin{cases} A_1\left(S-(1+s)K\right)^2; & S > (1+s)K \\ 0; & (1-s)K \le S \le (1+s)K \\ A_2\left(S-(1-s)K\right)^3; & S < (1-s)K \end{cases} \tag{4}$$

where A_1 and A_2 are remodeling constant, s is the width of lazy zone, K is the homeostatic stimulus for remodeling equilibrium. The exponents of bone formation and bone resorption are set to be 2 and 3, respectively, to simulate that resorption is a faster process than formation.

1.2.1.3 Bone remodeling based on daily effective stress

Carter et al. (1987) stated that a minimum amount of daily remodeling stimulus is required for bone maintenance (Carter et al., 1987; Beaupré et al., 1990). This daily remodeling stimulus (Ψ_b) characterizing the magnitude and cycles of loads is defined as,

$$\Psi_b = \left(\sum_{day} n_i \bar{\sigma}_i^{m}\right)^{1/m} \tag{5}$$

where n_i is the number of cycles of load type i, and m is an empirical constant to weight the relative importance of stress magnitude and number of load cycles, and $\bar{\sigma}_i$ is the continuum level effective stress, which is defined as,

$$\bar{\sigma}_i = \sqrt{2EU} \tag{6}$$

where E is the continuum average elastic modulus and U is the strain energy density. The velocity of surface remodeling in response to the daily remodeling stimulus was formulated as follows,

$$\dot{r} = \begin{cases} C_1\left(\Psi_b - \Psi_{bAS}\right) + \left(C_1 - C_2\right)w_1; & \Psi_b - \Psi_{bAS} < -w_1 \\ C_2\left(\Psi_b - \Psi_{bAS}\right); & -w_1 \le \Psi_b - \Psi_{bAS} < 0 \\ C_3\left(\Psi_b - \Psi_{bAS}\right); & 0 \le \Psi_b - \Psi_{bAS} \le w_2 \\ C_4\left(\Psi_b - \Psi_{bAS}\right) + \left(C_3 - C_4\right)w_2; & \Psi_b - \Psi_{bAS} > w_2 \end{cases} \tag{7}$$

where Ψ_{bAS} is the attractor stimulus for remodeling equilibrium, $C_1 - C_4$ are rate constants, and w_1 and w_2 are the boundaries of the normal activity region. Biologically, bone remodeling only occurs at the bone surface so the remodeling potential depends on the amount of available bone surface. Bone specific surface is used to quantify available bone surface for remodeling in bulk bone. The relation between the rate of density change and the rate of surface change can be expressed as,

$$\dot{\rho} = kS_v\rho_t\dot{r} \tag{8}$$

where k is the fraction of local area, which is actively remodeling, S_v is the bone-specific surface, which is determined according to apparent bone density (Martin, 1984), and ρ_t is the density of the fully mineralized tissue.

1.2.2 Modeling dental implant induced bone remodeling

Numerous clinical and histologic studies have been carried out to understand osseointegration in order to improve dental implant designs, surfaces and surgical protocols. Developing mathematical models of dental bone remodeling can help uncover biomechanical factors controlling short and long term survivability of implant treatments. Mathematical models mentioned previously were originally developed to study the phenomenon of bone adaptation to functional loads in long bone. However, simulations of bone remodeling in other bone regions such as acetabulum, proximal tibia, metacarpal, calcaneus and mandible (Carter & Beaupré, 2001; Pérez et al., 2010; Reina et al., 2007) have been reported. These long bone remodeling theories were used to study the bone remodeling, as a result of biomechanical alteration of the equilibrium state in the jaw bone due to use of dental implants (Lin et al., 2009a). Long term bone maintenance following fixed partial denture treatment was simulated by Field et al. (2010). A qualitative validation was reported by comparing the prediction of dental implant induced mandibular bone remodeling to clinical follow-up x-ray images over 48 months (Lin D. et al. 2010). Marginal bone loss is a common problem following dental implantation. Crupi et al. (2004), Li et al. (2007) and Lin C.-L. et al (2010) investigated the biomechanical causes of marginal bone loss by adding an overload bone loss criteria to remodeling equations. Lian et al. (2010) examined the effect of initial bone implant contact percentage on long term peri-implant bone remodeling and showed that 58-60% bone implant contact state develops at the equilibrium state no matter what initial contact percentage was assumed. Chou et al. (2011), investigated the effects of bone grafts in peri-implant bone remodeling in fresh extraction sockets and predicted that graft materials that are relatively stiff and that have high equilibrium stimulus values are likely to result in increased bone loss in the long term. In addition to studying clinical scenarios, factors influencing peri-implant bone remodeling is also of great interest to implant designers. A functionally graded dental implant, where the material composition varies from hydroxyapatite at the implant apex to titanium at the implant collar, was suggested. Lin et al. (2009b) predicted that the bone density can increase for implants made of functionally graded materials, but the initial stability of implant can be compromised due to the excessive vertical displacement due to the overall reduction in implant stiffness.

In Section 3, the strain energy density based remodeling theory (Section 1.2.1.2) is adopted to investigate the effects of various dental implant designs on bone remodeling. Equation (4) is first solved by the forward Euler time integration method, which gives,

$$\rho^{j+1} = \begin{cases} \rho^j + A_1\left(S^j - (1+s)K\right)^2 \Delta t; & S^j > (1+s)K \\ 0; & (1-s)K \le S^j \le (1+s)K \\ \rho^j + A_2\left(S^j - (1-s)K\right)^3 \Delta t; & S^j < (1-s)K \end{cases} \tag{9}$$

where j is the integration time step. Parameters A_1, A_2 and Δt can be treated as a single constant. To implement these formulations into finite element analysis, bone density must be related to material properties. The general relation of density and linear isotropic elasticity is,

$$E = C\rho^d \tag{10}$$

(Carter & Hayes, 1977), where E is the elastic modulus of bone. Empirical parameters C and d are set to be 3.79 and 3, respectively. The minimum modulus is 1 kPa. The maximum modulus is taken as 13 GPa, which corresponded to a density of 1.508 g/cm^3.

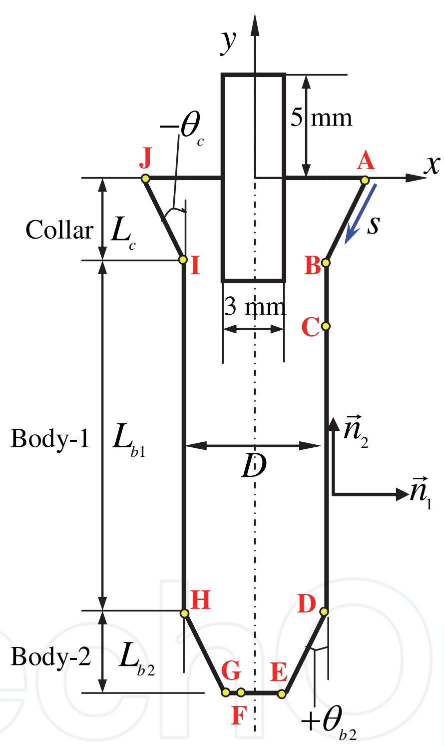

Fig. 1. The definitions of the parameters used to identify the contour of a generic dental implant.

2. Load transfer along the bone-implant interface

In order to investigate the nature of load transfer along the bone implant interface, a comprehensive parametric study of different implant designs was carried out. A generic implant with adjustable contour features, much like Faegh and Müftü (2010), was used. The normal and shear stress components, σ_{11} and σ_{12} acting normal and parallel to the implant surface, respectively, (Figure 1) were computed and plotted along the s-coordinate axis placed on the bone implant interface. Note that s = 0 represents the buccal-side and it is also marked as point-A, whereas point-J is the end of the interface path.

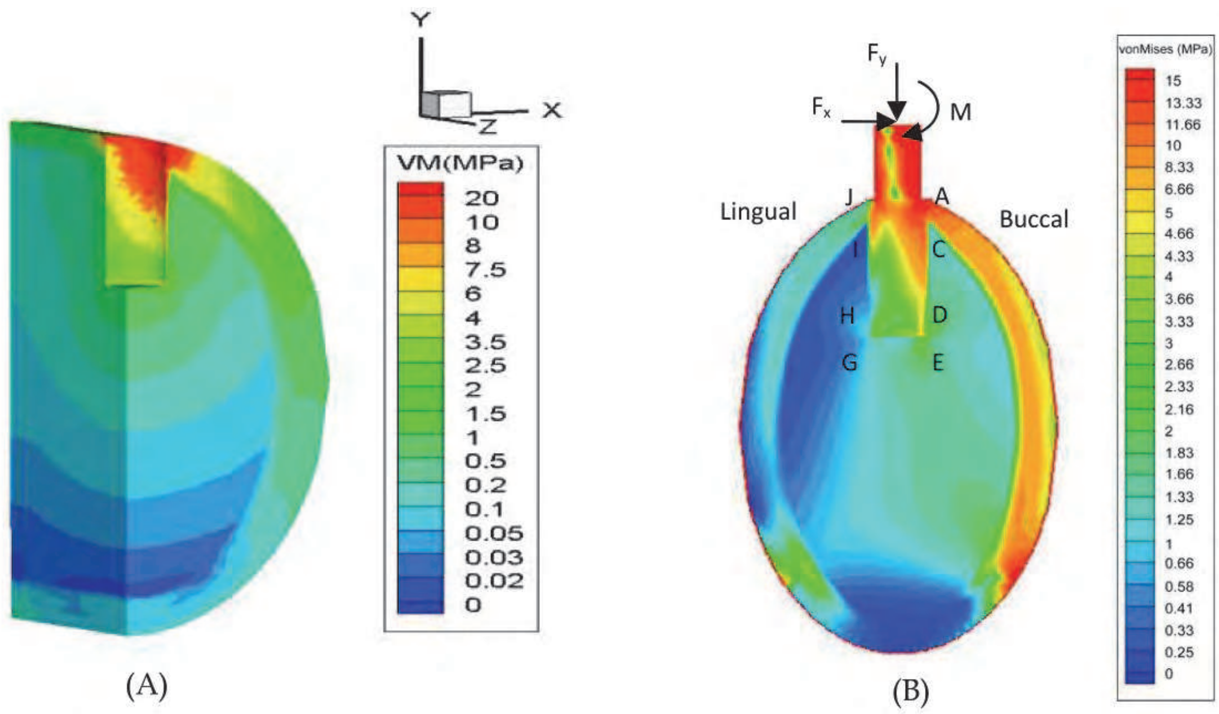

Fig. 2. von Mises stress distribtution in (A) the 3D model, (B) the 2D model.

2.1 Methods

Four main regions were designated to define implant geometry as the *collar*, *body*-1, *body*-2, and *apex* regions. The effects of the length, L_c, and slope, θ_c, of the collar region, the length, L_{b1}, and the diameter, D, of the body-1 region and the length, L_{b2}, and the slope, θ_{b2}, of the body-2 region were investigated. The apex was modeled to be flat. Faegh and Müftü (2010) investigated the effects of four common external thread shapes. The values they used were chosen according to the commercially available dental implants. Here we only report on the effect of a triangular thread shape, as the results and conclusions are similar. The thread geometry is defined by using three parameters. These are the *thread pitch*, p_t, the *thread depth* h_t, and the *thread slope* θ_t. The thread depth was h_t = 0.32 mm and the thread pitch was p_t = $L_{b1}/7$ in this study.

The implant-abutment connection was assumed to be monolithic; and, all of the components, (implant, abutment, cortical bone, and trabecular bone) were assumed to be perfectly bonded along their individual interfaces. The (x, y) coordinate system was placed at the center of the superior surface of the implant, as shown in Figure1 and the locations of the key points (A – J) on implant geometry, were programmed to be variable. In order to eliminate effects of bone morphology, which vary in individual jaws, the external geometry of bone was simplified as an ellipse. The major and minor axes of the bone model were idealized as 30 and 18 mm respectively, and a cortical layer of 2 mm was assumed.

Finite Element Method (FEM) was used and the system was modeled in ANSYS ver. 11 (Canonsburg, PA, USA). The analysis was carried out in 2D plane-strain. However, a 3D analysis was conducted to verify the level of validity of the 2D analysis. In 3D, the bone was modeled as an elliptical cylinder. The model was gradually meshed by creating extra regions around the implant with very high mesh density as in Faegh and Müftü (2010). 3D and 2D models were meshed with the structural solid elements, SOLID 185 and PLANE 42 of ANSYS respectively. An occlusal load of 113 N was applied at the center of abutment with the direction of 11 degrees with respect to the main axis, and a moment of 90 N.mm to mimic the biting force on the prosthesis. The elastic moduli of the implant system (Ti), the cortical bone, and the trabecular bone were set to 113, 13 and 1 GPa, respectively (Rieger et al., 1989a; Steinemann, 1996).

2.2 Results

Distribution of the von Mises stress in the bone, as predicted by 2D and 3D analyses, is presented in Figure 2, for a smooth faced implant with the dimensions θ_c = -10 degrees, L_c = 1 mm, L_{b1} = 5 mm, L_{b2} = 3 mm, θ_{b2} = 5 mm, D = 3.3 mm. This figure shows a reasonably similar stress distribution both in magnitude and trend. Close inspection of this figure also shows that: (i) Highest von Mises stress levels are observed on the buccal side of the cortical bone, and on the superior region of implant and abutment system; (ii) In general, the trabecular bone bears relatively low levels of stress compared to cortical bone; and, (iii) Higher von Mises stress is observed near the bone implant interface. Differences in the details of the 2D and 3D stress contours are due to the boundary conditions. In the 3D analysis, the bone was restricted at the distal ends, whereas in the 2D analysis the restriction is near the inferior periphery. This results in some distinct variations in regions away from the implant, as shown in the figure.

The effect of external thread shape on the von Mises stress distribution is presented for a smooth faced-implant and an externally threaded implant in Figure 3. The general contour parameters of these two cases are described above. This figure shows the load transfer along the bone-implant interface, via the normal σ_{11} and shear σ_{12} stresses. For the smooth (threadless) implant the normal stress σ_{11} is primarily compressive along the collar region and the apex of the implant, but it is small and tensile along the smooth faces of the body-1 and -2 regions. Jumps and stress concentrations are observed at the locations with abrupt changes in geometry and material properties. The collar region on the lingual side is seen to experience roughly 1/10th of the compressive stress experienced on the buccal side. Variation of the normal σ_{11} and shear σ_{12} stresses along the bone-implant interface for the externally threaded implant is presented in Figure 3B. It is observed that the interfacial normal and shear stresses increase around the external threads. In particular, on the first thread of the buccal side, where the thread is engaged with the cortical bone, a significant σ_{11} stress peak is observed. On the other hand, the general behavior of σ_{11} and σ_{12}, between the two implant types shows that the overall load transfer characteristics in the bone-implant interface are similar. It appears that at a local level the externally threaded implant is able to transfer higher loads to the tarbecular region. This can have significant effects on long term bone maintenance. Effects of different thread shapes are presented by Faegh & Müftü (2010).

The effects of different implant contours are investigated by changing the implant design parameters (θ_c, L_c, L_{b1}, L_{b2}, θ_{b2}, D) systematically (Table 1). Analysis of the interfacial stresses showed that the parameters that have the highest impact on the stress magnitude are the implant diameter D, the collar parameters θ_c and L_c, and the length of the body-1 region L_{b1}. The effects of these four parameters are summarized in Figure 4. Note that this analysis was carried out for smooth (threadless) implants. Figure 4 gives the maximum normal and shear stress values transferred to the bone. Incidentally all of the maximum values are found in the collar region of the buccal side. The results presented in Figure 4 are summarized as follows:

- For implants with larger diameter D the largest normal σ_{11} and shear stress σ_{12} transferred to the bone is reduced (Figures 4A-C).
- Increasingly negative collar slope (θ_c) causes the maximum normal stress transferred to the bone to increase, but it causes the maximum shear stress to decrease (Figure 4A).
- Increasing the length (L_c) of the collar and length (L_{b1}) of the body-1 regions cause the maximum normal stress and the maximum shear stress transferred to the bone to decrease (Figures 4B,C).

Length of Collar, L_c (mm)	1, 2
Angle of Collar, θ_c (degrees)	-10, -5, 0, 5, 10
Length of body-1, L_{b1} (mm)	4, 5, 6
Diameter of body-1, D (mm)	3.3, 3.5, 4
Length of body-2, L_{b2} (mm)	3, 4
Angle of body-2, θ_{b2} (degrees)	5, 10

Table 1. Implant dimensions that were varied in this work. See Figure 1 for the definitions of these variables. Note that θ_c as drawn in this figure is defined to be a negative angle, whereas θ_{b2} is defined to be positive.

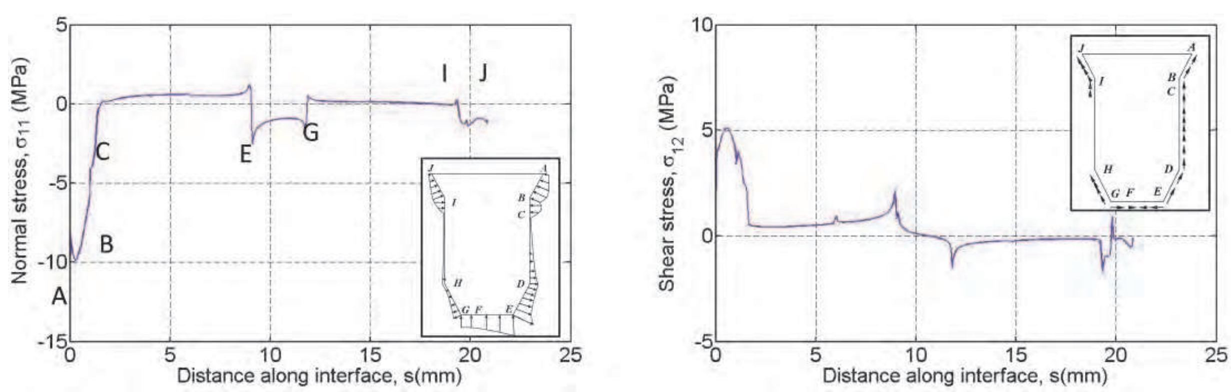

(A) σ_{11} and σ_{12} for smooth faced implant

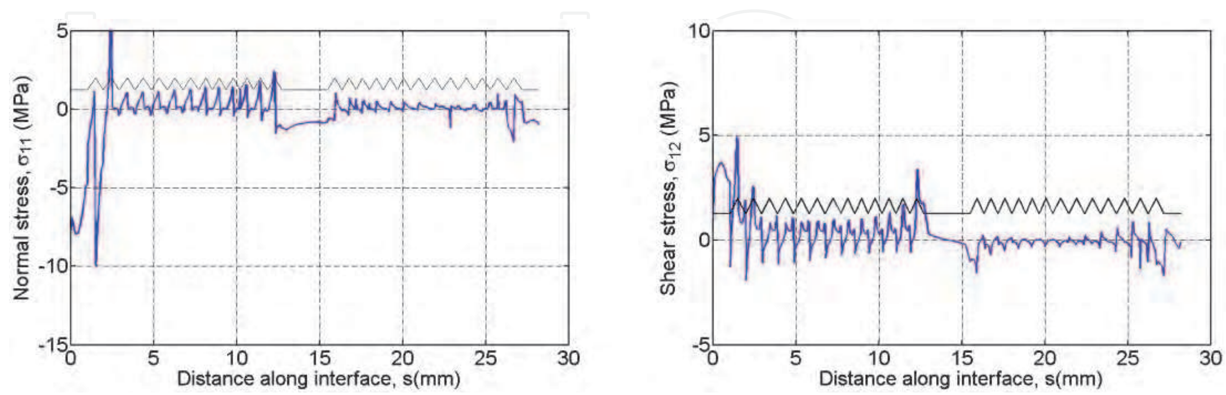

(B) σ_{11} and σ_{12} for externally threaded implant

Fig. 3. Normal and shear stresses along the interface for an implant with (A) no-external thread, and (B) triangular external thread. The other parameters of the implants are as follows: θ_c = -10 degrees, L_c = 1 mm and L_{b1} = 5 mm, L_{b2} = 3 mm, θ_{b2} = 5 degrees, D = 3.3 mm.

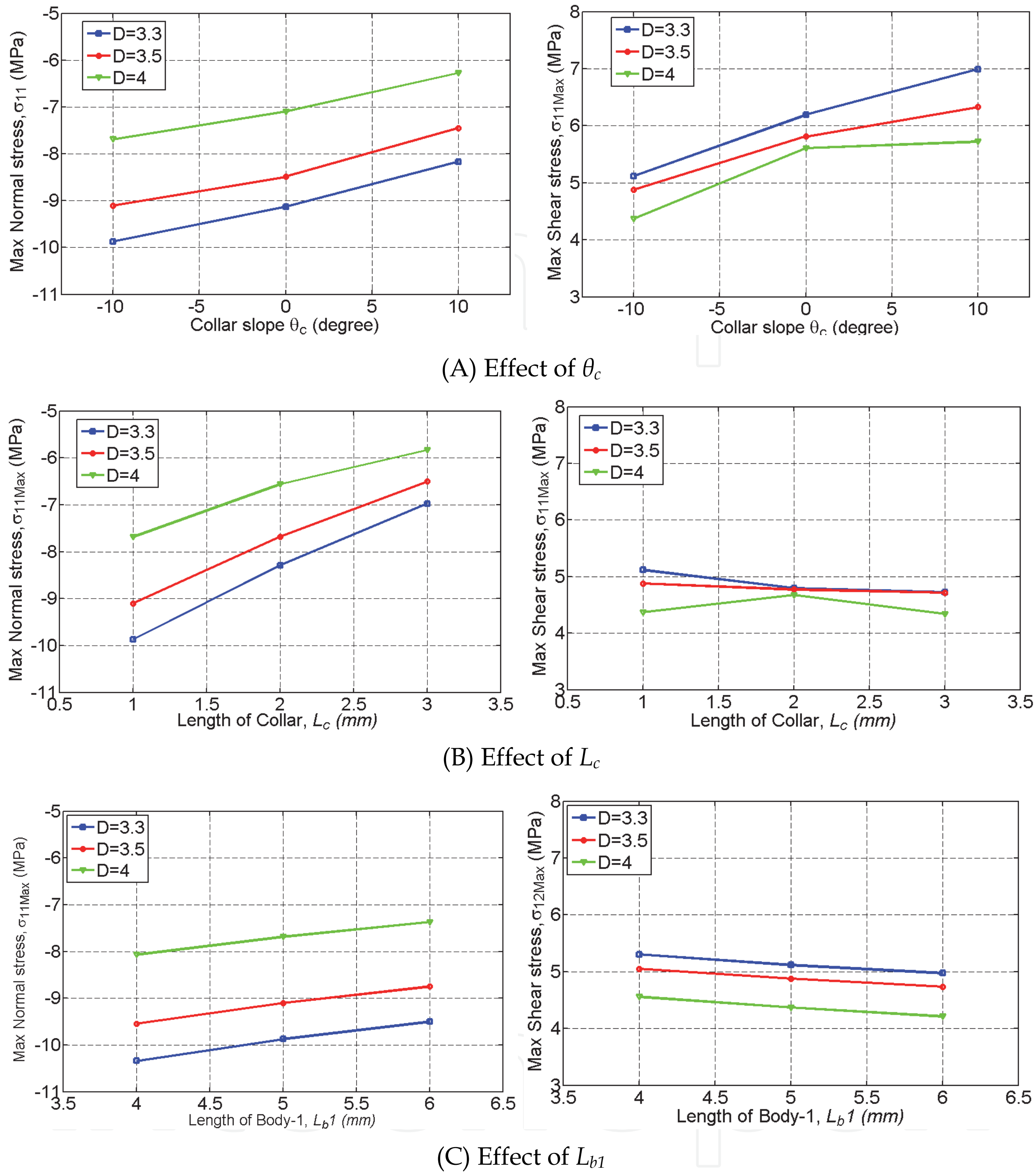

Fig. 4. Maximum normal and shear stress components σ_{11}, σ_{12} along the bone-implant interface with respect to contour parameter (A) collar slope, θ_c, (B) length of collar, L_c, (C) length of body-1, L_{b1}.

3. Simulation of dental implant induced bone remodeling

3.1 Methods

Bone remodeling around implant systems was modeled by using the remodeling theory presented by Huiskes and co-workers. Finite element method was used to assess the strain energy density in loading. Equations (9) and (10) were programmed into ANSYS. Two separate analyses are presented. The first one is a 2D plane strain analysis of bone remodeling originally presented by Chou et al. (2008), and the second one is a 3D analysis of bone remodeling by Chou et al. (2011). In the 2D analysis, the external bone contour of the mandible was obtained from a slice of CT scans at the premolar region in the buccal-lingual plane. A layer of cortical bone with a thickness of 1 mm was assigned. Elastic modulus and Poisson's ratio of this cortical layer are 13 GPa and 0.3, respectively. Dental implant systems considered were assumed to be made of titanium alloy (Ti-6Al-4V). Elastic modulus and Poisson's ratio are 113.8 GPa and 0.3 (Misch & Bidez, 1999), respectively. Quadrilateral elements were used to mesh the implant bone complex, and the bottom of mandible was constrained as shown in Figure 5. Occlusion was modeled as a concentrated force, F_o = 100 N, applied on the abutment in the buccal-lingual plane at 11° with respect to vertical axis (Chou et al., 2008). In addition, a uniform pressure (P_{mf} = 500 kPa) was assumed on the outer periphery of cortical bone to simulate the effect of mandibular flexure during jaw movement. Remodeling algorithm was applied only to the trabecular region, which was initially assumed to have a uniform density of 0.808 g/cm^3 corresponding to an elastic modulus of 2 GPa. Poisson's ratio was taken as 0.3. Remodeling parameters in Equation (9) were K = 25 J/kg, s = 0.65 and $A_i\Delta t$ = 5×10^{-3} for i = 1, 2.

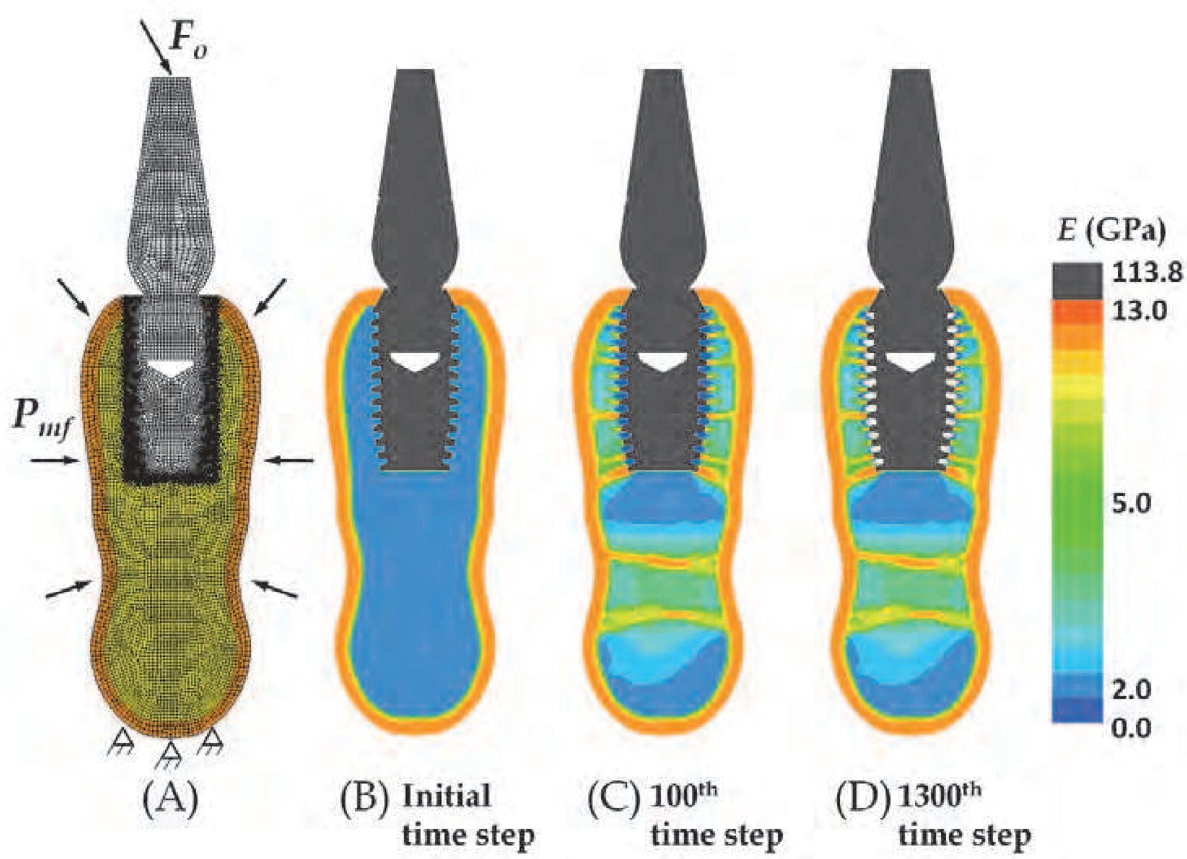

Fig. 5. (A) Two dimensional finite element mesh and loading conditions. Fine mesh is assigned at the bone implant interface. Elastic modulus distribution at (B) initial time step, (C) 100th time step, and (D) 1300th time step (Chou et al, 2008). (Printed with permission from Elsevier Limited).

3.2 Results and discussion

The transient change in the bone's elastic modulus at time steps 1, 100 and 1,300 is presented in Figure 5. This figure shows that the bone density, and hence the elastic modulus, changes gradually form a uniform initial state to a non-uniform state that is reflective of the local loading conditions. It is seen that high modulus bone is developed in the first 100 time steps, and no significant update takes place afterward. It is also observed that the tips of the external threads promote high density bone (high elastic modulus) but the area between the threads experience some bone resorption in the later stages of remodeling. As the Huiskes' model of bone remodeling doesn't have an effective means to handle actual time and loading rates, the time steps in this figure have arbitrary units. Nevertheless, one can see that bone density redistribution takes place quickly, but stays stable for prolonged loading.

Effects of four different implant contours on trabecular bone remodeling are presented in Figure 6. Three smooth faced implants systems and one externally threaded implant system are considered. Details of the geometrical differences are given in the figure. Cylindrical implant with the flat apex (Figure 6A) results in the largest amount of bone loss. The cylindrical implant with the rounded apex (Figure 6B) causes a similar response, albeit with less bone loss. The root form implant (Figure 6C) further reduces this bone loss region with the narrow apex design. For these three smooth faced implants, high density trabecular bone develops near the apical corners, and some high density struts emerging from the implant body are found in Figures 6A-6C. The main bodies of these implants fail to stimulate the bone sufficiently to induce significant bone remodeling. A study carried out by Watzak et al. (2005) in baboons investigates the effects of surface features such as threads and chemical modifications to the surface also show similar results. Note the lack of tarbecular bone under the flat apex of the implant in Figure 6A. Watzak et al. (2005) also indicate that signs of bone remodeling at the surface of cylindrical implant were absent.

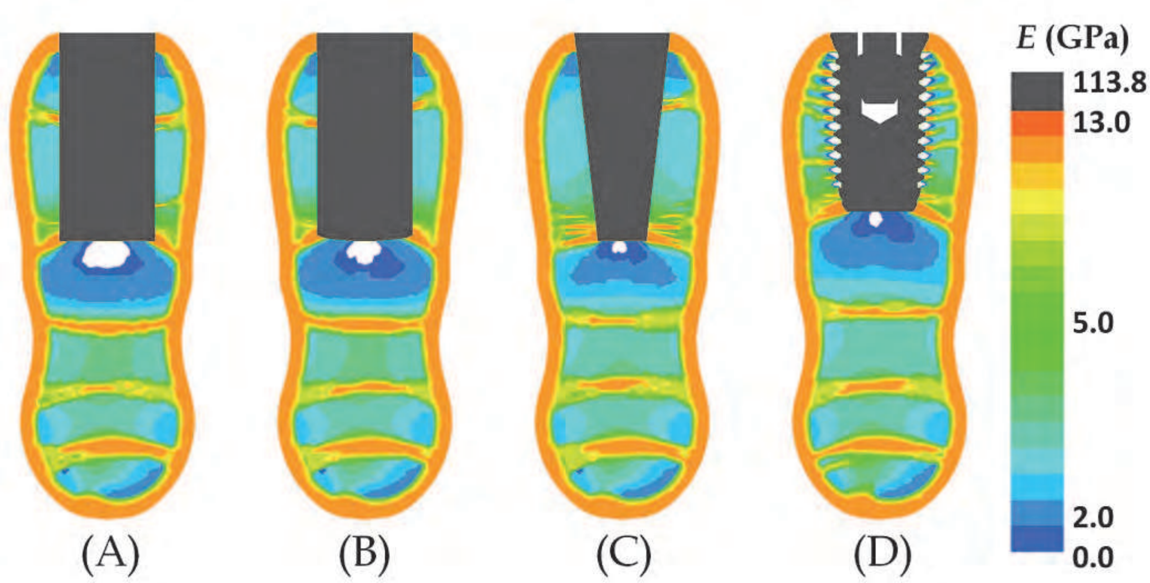

Fig. 6. Elastic modulus distribution predicted around a (A) cylindrical implant, a (B) cylindrical implant with rounded apex, a (C) root from implant and a (D) threaded implant. (Chou et al., 2008). (Printed with permission from Elsevier Limited).

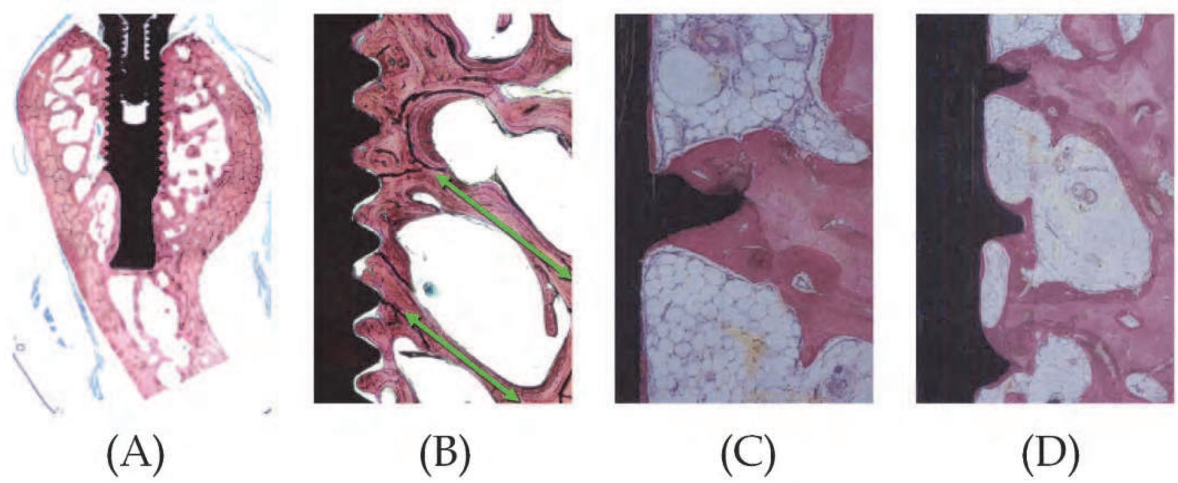

Fig. 7. Histologic studies show (A) bone remodeling around dental implant (Watzak et al., 2005), (B) trabeculae like dense struts at implant surface (Watzak et al., 2005), (C) and (D) bone growth around implant threads (Schenk & Buser, 1998). (Printed with permission from John Wiley and Sons.)

The predictions for the externally threaded implants (Figures 5D and 6D) are significantly different from smooth faced implants. In the case of threaded design, development of high density bone around the threads is evident. Similar remodeling patterns were reported in the histologic observations of Watzak et al. (2005) in Figures 7A and 7B, and those of Schenk & Buser (1998) in Figures 7C and 7D. Note that while Figures 7B-7D show bone density increase around the threads some resorption is also observed between the threads in Figures 7C and 7D similar to our simulations.

In the study presented above, the homeostatic stimulus, K, was assumed to be constant. Although satisfying results were predicted by this simplification, it implies that bone remodels toward a spatially homogenous biomechanical field, despite the fact that the biological environment (i.e. the cells and the nutrients) varies among bone sites. In order to address this issue, we used a site dependant homeostatic stimulus, $K(x,y,z)$ in a 3D analysis of bone remodeling around a dental implant. This approach was also used by Huiskes et al. (1992) and Weinans, et al. (1993) to simulate bone remodeling around hip prostheses. In addition, we hypothesize that the site specific homeostatic stimulus must be similar to that induced by a natural tooth in its supporting bone. Therefore, the site-specific K value was computed, first for a model with a natural tooth that is shown in Figure 8A. These K values were subsequently used for predicting the bone remodeling around a dental implant system. Details are presented by Chou et al. (2011).

A three-dimensional mandibular segment was constructed from the CT-scan of the premolar region of the mandible. Same material properties and occlusal load, as above, were applied to the finite element models of bone tooth and bone implant prosthesis complexes shown in Figure 8. The elastic modulus of the tooth and the prosthesis were taken as 20 GPa and 80 GPa, respectively; and the Poisson's ratios were assumed to be 0.3. Similar to clinical practice, the interstitial gap created by the incongruence of dental implant with extraction socket is filled with a (virtual) bone graft in the finite element model. The elastic modulus of the graft was set to be the same as trabecular bone. The mandible segment was constrained in all directions on the distal buccal-lingual plane, and symmetry boundary condition was applied to the mesial buccal-lingual plane shown in Figure 8.

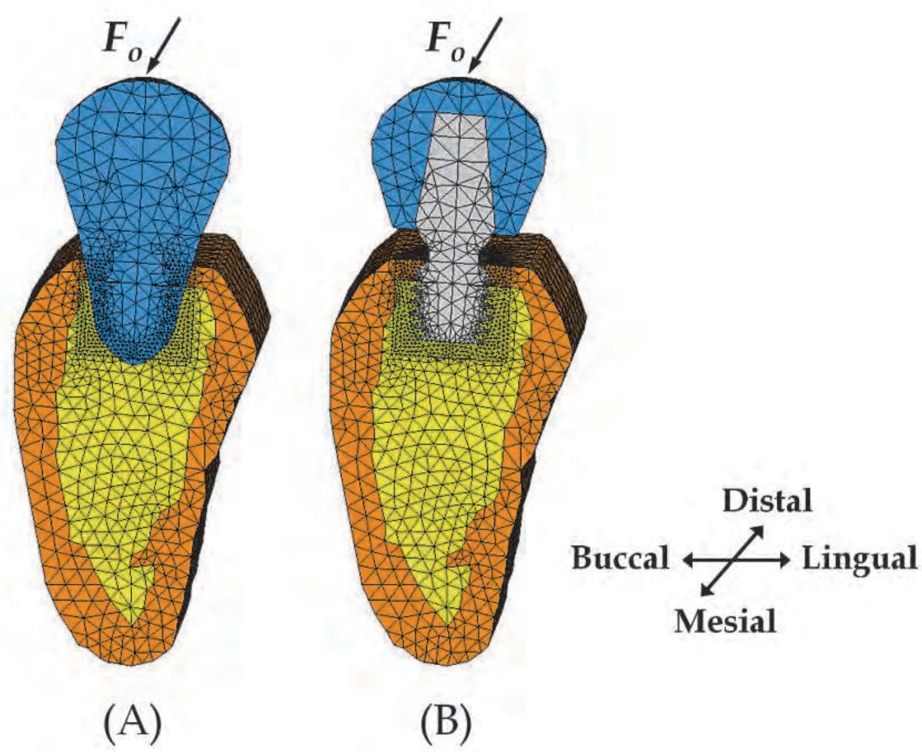

Fig. 8. Finite element models of (A) bone tooth and (B) bone implant prosthesis complexes. A concentrated force F_o is used to simulate occlusion.

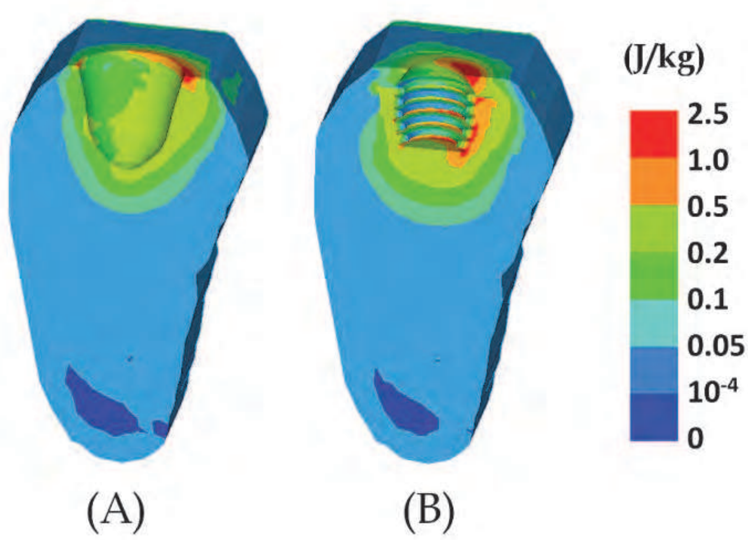

Fig. 9. (A) Homeostatic stimuli distribution in bone induced by tooth. (B) Remodeling stimuli distribution in bone induced by dental implant prior to bone remodeling (Initial time step).

The site dependant homeostatic stimuli K was based on the strain energy per unit bone mass, induced by the occlusal force acting on the natural tooth. Next, homeostatic stimuli in the graft region had to be assumed. This assumption was based on the stimulus levels near the tooth. Therefore, a constant value K_g = 0.25 J/kg was used to represent the homeostatic stimulus of the bone graft. This parameter is treated as the potential of bone graft to induce

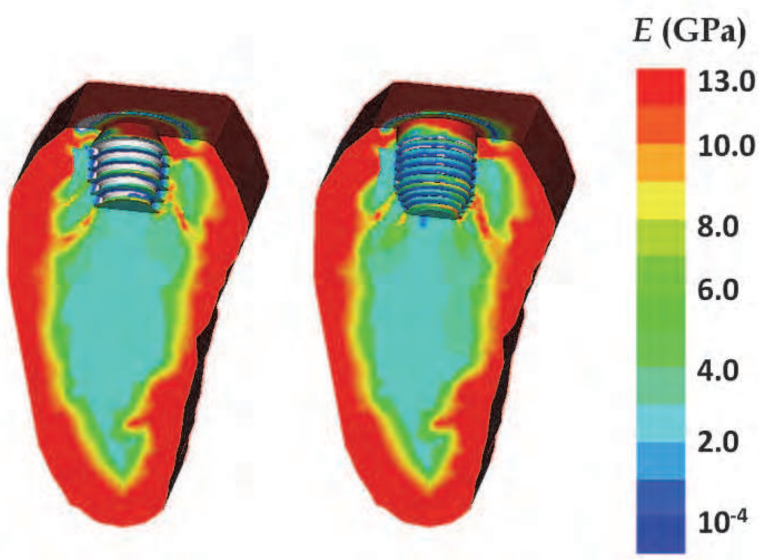

Fig. 10. Elastic modulus distribution predicted around two different implant designs at remodeling equilibrium.

bone remodeling (Chou et al., 2011). Figure 9A shows the computed site specific *K* distribution, and Figure 9B shows the initial remodeling stimuli *S* distribution around the implant It is seen that the variations of the homeostatic stimuli *K*. It is seen that the homeostatic stimuli *K* and the remodeling stimulus *S* are localized around the tooth and the dental implant. In fact, it can be stated that a certain degree of biomimetic match has been obtained in this case. For implants with longer body-1 and body-2 regions, the remodeling stimulus is markedly different than that of the tooth (Chou et al., 2011).
Figure 10 shows the elastic modulus distribution at remodeling equilibrium for two wide-diameter, short implants with different thread profiles. Trabeculae like dense bone struts develop at the implant surface and extend toward cortical layer. Implant threads show same characteristics as in 2D analysis; bone apposition occurs at the thread tips, and the regions between the implant threads are prone to bone resorption. The predicted results also demonstrate that bone remodeling is a localized event, and it decays with increasing distance away from implant surface. A histologic study by Coelho et al. (2009) reported high levels of osteoactivity taking place near the implant surface. This can be observed in the predictions in Figure 10.

4. Summary and conclusions

Dental implants provide an attractive alternative to classical prosthodontic techniques in the treatment of edentulism. It has been shown clinically that the bone loss after tooth extraction is reversed by the placement of dental implant, since the first human study reported by Brånemark et al. (1977). The mechanical loads exerted by occlusion are transferred into jawbone through the dental implant, and can potentially affect the bone remodeling according to Wolff's law (Wolff, 1892). Therefore, it is critical to develop a sound understanding of the load transfer mechanism from the implant to the bone. It is equally important, to supply a dental implant with critical chemical and contour features on its surface. If the ideal load transfer characteristics can be identified, it may be possible to improve the osseointegration.

A systematic analysis of the load transfer along the bone-implant interface was carried out by using finite element analysis. Various implant systems were designed by changing their contour parameters. Among all design parameters, the diameter, the collar slope, the collar length and the length of the implant were found to be the most influential parameters to the interfacial variations of the normal and shear stresses. Maximum normal and shear stresses were found to occur on the buccal side of the cortical bone, as in many other studies. It was shown that both maximum normal and shear stress values can be reduced by either widening the implant diameter, or increasing the lengths of the collar and body regions. Varying the slope of the collar from negative to positive was found to increase the maximum normal stress, but to reduce the maximum shear stress transferred along the interface. The effects of the external threads were also investigated. It was seen that the general interfacial load transfer behavior doesn't change with respect to smooth faced implants, but locally the interfacial stresses are elevated around the threads. A bone remodeling algorithm was implemented to analyze the bone maintenance characteristics of smooth faced and threaded implants. This showed poor bone maintenance around smooth faced implants. On the other hand, significant remodeling and densification was predicted around threaded implants. It was shown that the thread tips promote the development of dense bone. Total bone resorption was predicted in the areas between the threads. Similar remodeling phenomenon around implant threads was reported in histologic studies by Schenk & Buser (1998) and Watzak et al. (2005). It appears that adequately high interfacial stresses are introduced by using externally threaded implants.

This study contributes to our understanding of the complex problem of load transfer mechanism in the bone-dental implant interface and the subsequent peri-implant bone remodeling. Despite the interesting conclusions drawn from the results, the computational predictions are still limited by the assumptions and simplifications of loading, geometry and material properties made in this study.

5. References

Akça, K., Iplikçioğlu, H. (2001). Finite element stress analysis of the influence of staggered versus straight placement of dental implants. *The International Journal of Oral & Maxillofacial Implants*, Vol.16, No.5, (Sep-Oct 2001 Sep-Oct), pp. 722-30

Aparicio, C., Orozco, P. (1998). Use of 5 mm diameter implants: Periotest values related to a clinical and radiographic evaluation. *Clinical Oral Implants Research*, Vol.9, No.6, (Dec 1998), pp. 398-406

Bahat, O., Handelsman, M. (1996). Use of wide implants and double implants in the posterior jaw: a clinical report. *The International Journal of Oral & Maxillofacial Implants*,Vol.11, No.3, (May-Jun 1996), pp. 379-86

Balshi, T.J., Wolfinger, G.J. (1997a). Immediate loading of branemark implants in edenulous mandibles: a preliminary report. *Implant Dentistry [Implant Dent]*, Vol.6, No.2, (Summer 1997), pp. 83-8, ISSN: 1056-6163

Balshi, T.J., Wolfinger, G.J. (1997b). Two implant supported single molar replacement: interdental space requirements and comparison to alternative options. *The International Journal of Periodontics & Restorative Dentistry*, Vol.17, No.5, (Oct 1997), pp. 426-35

Beaupre, G.S., Orr, T.E. & Carter, D.R. (1990). An approach for time-dependent bone modeling and remodeling-theoretical development. *Journal of Orthopaedic Research*, Vol. 8, No. 5, (September 1990), pp. 651-661, ISSN 1554-527X

Bidez, M.W., Stephens, B.J., Lemons, J.E. (1988). A comparison of interfacial assumptions in a three dimensional stress analysis of a CP-Ti dental implant system, *Transactions Third World Biomaterials Congress*, 117, Kyoto, Japan, 1988

Blatz, M.B., Strub, J.R., Glaser, R., Beghart, W. (1998). Use of wide-diameter and standard diameter implants to replace single molars: Two case presentations. *Int J Proshodont*, Vol. 11, pp. 356-363

Borchers, L., Reichart, P. (1983). Three-dimensional stress distribution around a dental implant at different stages of interface development. *J. Dent. Res.*, Vol.62, No.2, pp. 155-9

Bozkaya, D., Müftü, S., Müftü, A. (2004). Evaluation of Load Transfer Characteristics of Five Different Implants in Compact Bone at Different Load Levels by Finite Element Analysis, *Journal of Prosthetic Dentistry*, Vol. 92, No. 6 pp. 523-530

Brånemark, P.I., Hansson, B.O., Adell, R., Breine, U., Lindström, J., Hallén, O. & Ohman, A. (1977). Osseointegrated implants in the treatment of endentulous jaw. Experience from a 10-year period. *Scandinavian Journal of Plastic and Reconstructive Surgery Supplementum*, Vol. 16, pp. 1-132, ISSN 0581-9474

Brånemark, P.I., Engstrand, P., Ohrnell, L.O., Gröndahl, K., Nilsson, P., Hagberg, K., Darle, C., Lekholm, U. (1999) Branemark Novum: a new treatment concept for rehabilitation of the edenrulous mandible. Preliminary results from a prospective clinical follow-up study. *Clinical Implant Dentistry And Related Research*, Vol.1, No.1, pp. 2-16

Brånemark, P.I., Zarb, G., Alberktsson, T. (1985). Tissue Integrated Prostheses, Quintessence, Chicago

Brunski, J.B. (1999). In vivo bone response to biomechanical loading at the bone/dental-implant interface. *Adv Dent Res 1999*. Vol.13, pp. 99-119

Canay, S., Hersek, N., Akpinar, I., Aşik, Z. (1996). Comparison of stress distribution around vertical and angled implants with finite element analysis. *Quintessence International (Berlin, Germany: 1985)*, Vol.27, No.9, 591-8

Carda, C., Silvestrini, G., Gomez de Ferraris, M.E., Peydró, A. & Bonucci, E. (2005). Osteoprotegerin (OPG) and RANKL expression and distribution in developing human craniomandibular joint. Tissue and Cell, Vol. 37, No. 3, (Jun 2005), pp. 247-255, ISSN 0040-8166

Carter, D.R., Fyhrie, D.P. & Whalen, R.T. (1987). Trabecular bone dnsity and loading history: regulation of connective tissue biology by mechanical energy. *Journal of Biomechanics*, Vol. 20, No. 8, pp. 785-794

Carter, D.R. & Beaupré, G.S. (2001). *Skeletal Function and Form: Mechanobiology of Skeletal Development, Aging, and Regeneration*. Cambridge University Press, ISBN 052179000X, New York

Carter D.R., Hayes W.C. (1977).The behavior of bone as a two-phase porous structure. *J. Bone Joint Surg*. Vol. 59A, pp. 954-962

Chou, H.-Y., Jagodnik, J. & Müftü, S. (2008). Predictions of bone remodeling around dental implant systems. *Journal of Biomechanics*, Vol. 41, No. 6, (April 2008), pp. 1365-1373, ISSN 0021-9290

Chou, H.-Y., Müftü, S. & Bozkaya, D. (2010). Combined effects of implant insertion depth and alveolar bone quality on periimplant bone strain induced by a wide-diameter, short implant and a narrow-diameter, long implant. *The Journal of Prosthetic Dentistry*, Vol. 104, No. 5, (November 2010), pp. 293-300, ISSN 0022-3913

Chou, H.-Y., Romanos, G., Müftü, A. & Müftü, A. (2011). Peri-Implant Bone Remodeling Around a Fresh Extraction Socket: Predictions of Bone Maintenance by Finite Element Method, *International Journal of Oral and Maxilliofacial Implants*, in review.

Coelho, P.G., Cardaropoli, G., Suzuki, M. & Lemons, J.E. Histomorphometric evaluation of a nanothickness bioceramic deposition on endosseous implants: a study in dogs. (2009). Clinical Implant Dentistry Res, Vol. 11, No. 4, (December 2009), pp. 292-302 ISSN 1708-8208

Chow, J., Hui, E., Liu, J., Li, D., Wat, P., Li, W., Yau, Y.K., Law, H. (2001). The Hong Kong Bridge Protocol. Immediate loading of mandibular branemark fixures using a fixed provisional prosthesis: preliminary results. *Clin Implant Dent Relat Res*, Vol.3, No.3, pp. 166-74

Chun, H.J., Cheong, S.Y., Han, J.H., Heo, S.J., Chung, J.P., Rhyu, I.C., Choi, Y.C., Baik, H.K., Ku, Y., Kim, M.H. (2002). Evaluation of design parameters of osseointegrated dental implants using finite element analysis. *J Oral Rehabil*, Vol.29, No.6, pp. 565-574

Cook, S.D., Klawitter, J.J., Weinstein, A.M. Lavernia, C.J. (1980). The design and evaluation of dental implants with finite element analysis, In: *Finite Elements in Biomechanics.*, R.A. Gallagher, (Ed.), 159-168, University of Arizona Press, Tuscon, AZ

Cook, S.D., Klawitter, J.J., Weinstein, A.M. (1982a). The influence of implant geometry on the stress distribution around dental implants. *J. Biomed. Mater. Res.,* Vol.16, No.4, pp. 369-79

Cook, S.D., Weinstein, A.M., Klawitter, J.J. (1982b). Parameters affecting the stress distribution around LTI carbon and aluminum oxide dental implants. *J. Biomed. Mater. Res.*, Vol.16, No.6, pp. 875-85

Crupi, V., Guglielmino, E., La Rosa, G., Vander Sloten, J. & Van Oosterwyck, H. (2004). Numerical analysis of bone adaptation around an oral implant due to overload stress. *Proceedings of the Institution of Mechcanical Engineers. Part H: Journal of Engineering in Medicine*. Vol. 218, No. 6, pp. 407-415, ISSN 0954-4119

Davarpanah, M., Martinez, H., Kebir, M., Etienne, D., Tecucianu, J.F. (2001). Wide diameter implants: new concepts. The *International Journal of Periodontics & Restorative Dentistry,* Vol. 21. No.2, (Apr 2001), pp. 149-59, ISSN 0198-7569

Duyck, J., Naert, I.E., Van Oosterwyck, H., Van der Sloten, J., De Cooman, M., Lievens, S., Puers, B. (1997). Biomechanics of dental implant: a review of the literature. *Technology and Health care 1997*, Vol.5, pp. 253-273

Ericsson, I., Nilson, H., Lindh, T., Nilner, K., Randow, K. (2000). Immediate functional loading of branemark single tooth implants. An 18 months' clinical pilot follow-up study. *Clinical Oral Implants Research*, Vol.11, No.1 (February 2000), pp. 26-33

Faegh, S., Müftü, S. (2010). Load transfer along the bone-dental implant interface. *Journal of Biomechanics*, Vol. 43, pp. 1761-1770

Farah, J.W., Craig, R.G., Yapp, R.A. (1979-80). Stress distribution caused by blade type implant. *Implantologist*, 1979-80; Vol.1, No.4, pp. 77-86

Field, C., Li, Q., Li, W., Thompson, M. & Swain, M. (2010). Prediction of mandibular bone remodelling induced by fixed partial dentures. *Journal of Biomechanics*, Vol. 43, No. 9, (March 2010), pp. 1771-1779, ISSN 0021-9290

Frandsen, P.A., Christoffersen, H., Madsen, T. (1984). Holding power of different screws in the femoral head. A study in hyman cadaver hips. *Acta Orthopaedica Scandinavica*, Vol.55, No.3, (Jun 1984), pp. 349-51

Frost, H.M. (1987). Bone "mass" and the "mechanostat": a proposal. *The Anatomical Record*, Vol. 219, No. 1, (September 1987), pp. 1-9, ISSN 1932-8486

Frost, H.M. (2003). Bone's mechanostat: a 2003 update. *The Anatomical Record*, Vol. 275A, No. 2, (December 2003), pp. 1043-1121, ISSN 1932-8486

Geng, J.P., Tan, K.B., Liu, G.R. (2001). Application of finite element analysis in implant dentistry: a review of the literature. *J Prosthet Dent*, Vol.85, No.6, pp. 585-598

Geramy, A., Morgano, S.M. (2004). Finite element analysis of three designs of an implant-supported molar crown. *The Journal of Prosthetic Dentistry*, Vol.92, No.5, pp. 434-40

Graves, S.L., Siddiqui, A.A., Jansen, C.E., Beaty, K.D. (1994). Wide diameter implants: Indications, considerations and preliminary results over a two-year period. *Australian prosthodontic Journal*, Vol.8, pp. 31-37

Griffin, T.J., Cheung, W.S. (2004). The use of short, wide implants in posterior area with reduced bone height: a retrospective investigation. *The Journal of Prosthetic Dentistry*, Vol.92, No.2, (Aug 2004), pp. 139-44

Gross, M., Laufer, B.Z. (1997). Splinting osseointegrated implants and natural teeth in rehabilitation of partially edentulous patients. Part I: laboratory and clinical studies. *Journal Of Oral Rehabilitation*, Vol.24, No.11, (Nov 1997), pp. 863-70

Hansson, S. (1999). The implant neck: smooth or provided with retention elements: A biomechanical approach. *Clinical Oral Implants Research*, Vol.10, No.5, pp. 394-405

Hart, R..T. (2001). Bone modeling and remodeling: theories and computation, In: *Bone Mechanics Handbook* (2nd edition), Cowin, S.C., (Ed.), 31_1-31_42, CRC Press, ISBN 0849391172, Boca Rotan, FL

Holmgren, E.P., Seckinger, R.J., Kilgren, L.M., Mante, F. (1998). Evaluating parameters of osseointegrated dental implants using finite element analysis-a two dimensional comparative study examining the effects of implant diameter, implant shape, and load direction. *The Journal of Oral Implantology*, Vol.24, No.2, pp. 80-8

Hipp, J.A., Brunski, J.B., Shephard, M.S., Cochran, G.V.B. (1985). Finite element models for implants in bone: interfacial assumptions, In: *Biomechanics, Current Interdisciplinary Research,* 447-452, E. Schneider and S.A. Perren. M. Nijhoff, (Ed.), Dordrecht, The Netherlands

Huang, H.-L, Hsu, J.-T., Fuh L.-J., Lin, D.-J. & Chen, M.Y.-C., (2010). Biomechanical simulation of various surface roughnesses and geometric designs on an immediately loaded dental implant. *Computers in Biology and Medicine*, Vol.40, No.5, pp. 525-532

Huang, S.-C. & Tsai, C.-F. (2003). Finite element analysis of a dental implant. *Biomedical Engineering: Applications, Basis and Communications*, Vol. 15, No. 2, pp. 82-85

Huiskes, R., Weinans, H., Grootenboer, H.J., Dalstra, M., Fudala, B. & Sloof, T.J. (1987). Adaptive bone remodeling theory applied to prosthetic-design analysis. *Journal of Biomechanics*, Vol. 20, No. 11-12, pp. 1135-1150, ISSN 0021-9290

Huiskes, R., Weinans, H. & van Rietbergen, B. (1992). The relationship between stress shielding and bone resorption around total hip stems and the effects of flexible materials. *Clinical Orthopaedics and Related Research*, Vol. 274, (January 1992), pp. 124-134, ISSN 0009-921X

Iplikcioglu, H., Akca, K. (2002). Comparative evaluation of the effect of diameter, length and number of implants supporting three-unit fixed partial prostheses on stress distribution in the bone. *J Dent*, Vol.30, No.1, pp. 41-46

Jaffin, R.A., Kumar, A., Berman, C.L. (2000). Immediate loading of implants in partially and fully edentulous jaws; a series of 27 case reports. *Journal of Periodontology*, Vol.71, No.5, (May 2000), pp. 833-8

Jarvis, W.C. (1996). Know when to use wide bodied implants to limit bone stress. *Dental Implantology Update*, Vol.7, No.12, (Dec 1996) pp. 89-92

Jarvis, W.C. (1997). Biomechanical advantage of wide diameter implants. *Compendium of Continuing Education In Dentistry (Jamesburg, N.J.: 1995)*, Vol.18, No.7, (Jul 1997), pp. 687-92

Kinni, M., E., Hokama, S. N., Caputo, A.A. (1987). Force transfer by osseointegration implant devices. *Int. J. Oral Maxillofac. Implants*, Vol.2, No.1, pp. 11-14

Kitoh M., Suetsugu T., Murakami Y., Tabata T. (1978). A biomathematical study on implant desing and stress distribution. *The Bulletin Of Tokyo Medical And Dental University*, Vol.25, No.4, pp. 269-76

Kong, L., Sun, Y., Hu, K., Liu, Y., Li D., & Liu, B. (2008). Selections of the cylinder implant neck taper and implant end fillet for optimal biomechanical properties: A three-dimensional finite element analysis. *Journal of Biomechanics*, Vol. 41, No. 5, pp. 1124-1130

Langer, B., Langer, L., Herrmann, I., Jorneus, L. (1993). The wide fixture: a solution for special bone situation and a rescue for the compromised implant. *The International Journal of Oral & Maxillofacial Implants*, Vol.8, No.4, pp. 400-8

Lavernia, C.J., Cook, S.D., Weinstein, A.M., Llawitter, J.J. (1981). An analysis of stresses in a dental implant system. *J. Biomech.*, Vol.14, No.8, pp. 555-60

Lavernia, C.J., Cook, S.D., Weinstein, A.M., Klawitter, J.J. (1982). The influence of the bone-implant interface on stress profiles surrounding Al_2O_3 and carbon implants. *Ann. Biomed. Engng*, Vol.10, No.3, pp. 129-38

Lazzara, R.J. (1994). Criteria for implant selection: Surgical and prosthetic considerations. *Pract Peno & Aest Dent* Vol.6, No.9, pp, 62

Lekholm U., Zarb G.A. (1985) Patient selection and preparation. In: *Tissue-integrated prostheses: osseointegration in clinical dentistry*, Brånemark P.I., Zarb G.A., Albrektsson T., (Ed.), Quintessence, Chicago, pp. 199-209

Leucht, P., Kim, J.B., Wazen, R., Currey, J.A., Nanci, A., Brunski, J.B. & Helms, J.A. (2007). Effect of mechanical stimuli on skeletal regeneration around implants. *Bone*, Vol. 40, No. 4, (April 2007), pp. 919-930, ISSN 8756-2382

Li, J., Li, H., Shi, L., Fok, A.S.L., Ucer, C., Devlin, H., Horner, K. & Silikas, N. (2007). A mathematical model for simulating the bone remodeling process under mechanical stimulus. *Dental Materials*, Vol. 23, No. 9, (November, 2006), pp. 1073-1078, ISSN 0109-5641

Li, T., Hu, K., Cheng, L., Ding, Y., Ding, Y., Shao, J. & Kong, L., (2011). Optimum selection of the dental implant diameter and length in the posterior mandible with poor bone quality - A 3D finite element analysis. *Applied Mathematical Modelling*, Vol. 35, No.1, pp. 446-456

Lian, Z., Guan, H., Ivanovski, S., Loo, Y.-C., Johnson, N.W. & Zhang, H. (2010). Effect of bone to implant contact percentage on bone to implant contact percentage on bone remodelling surrounding a dental implant. *International Journal of Oral and Maxillofacial Surgery*, Vol. 39, No. 7, (July 2010), pp. 690-698, ISSN 0901-5027

Lin, D., Li, Q., Li, W. & Swain , M. (2009a). Dental implant induced bone remodeling and associated algorithms. *Journal of the Mechanical Behavior of Biomedical Materials*, Vol. 2, No. 5, (December 2008), pp. 410-432, ISSN 1751-6161

Lin, D., Li, Q., Li, W., Zhou, S. & Swain, M.V. (2009b). Design optimization of functionally graded dental implant for bone remodeling. Composites Part B: Engineering, Vol. 40, No. 7, (October 2009), pp. 668-675, ISSN 1359-8368

Lin, D., Li, Q., Li, W., Duckmanton, N. & Swain, M. (2010). Mandibular bone remodeling induced by dental implant. *Journal of Biomechanics*, Vol. 43, No. 2, (January 2010), pp. 287-293, ISSN 0021-9290

Lin, C.-L., Lin, Y.-H. & Chang, S.-H. (2010). Multi-factorial analysis of variables influencing the bone loss of an implant placed in the maxilla: prediction using FEA and SED bone remodeling algorithm. *Journal of Biomechanics*, Vol. 43, No. 4, (November 2009), pp. 644-651, ISSN 0021-9290

Mahon, J.M., Norling, B.K., Phoenix, R.D. (2000). Effects of varying fixture width on stress and strain distribution associated with an implant stack system. *Implant Dentistry*, Vol.9, No.4, pp. 310-20

Martin, R.B. (1984). Porosity and specific surface in bone. *Critical Reviews in Biomedical Engineering*, Vol. 10, No. 3, pp. 179-222, ISSN 0278-940X

Martin, R.B., Burr, D.B. & Sharkey, N.A. (1998). *Skeletal Tissue Mechanics*. Springer, ISBN 0387984747, New York

Marx, R.E. (2007). Bone and bone graft healing. *Oral and Maxillofacial Surgery Clinics of North America*, Vol. 19, No. 4, (November 2007), pp. 455-466, ISSN 1042-3699

Meijer, H.J., Starmans, F.J., Steen, W.H., Bosman, F. (1994). A three-dimensional finite element study on two versus four implants in an edentulous mandible. *The International Journal of Prosthodontics*, Vol.7, No.3, (May-Jun 1994), pp. 217-9

Misch, C.E., Hoar, J., Beck, G., Hazen, R., Misch, C.M. (1998). A bone quality based implant system: a preliminary report of stage I & stage II. *Implant Dentistry*, Vol.7, No.1, pp. 35-42

Misch, C.E., Dietsh-Misch, F., Hoar, J., Beck, G., Hazen, R., Misch, C.M. (1999). A bone quality based implant system: first year of prosthetic loading. *The Journal of Oral Implantology*, Vol.25, No.3, pp. 185-97

Misch, C.E. (1999a). Implant design considerations for the posterior regions of the mouth. *Implant Dentistry*, Vol.8, No.4, pp. 376-86

Misch, C.E. (1999b). *Contemporary Implant Dentistry*, Mosby, St. Louis

Misch, C.E. & Bidez, M.W. (1999). A scientific rationale for dental implant design, In: *Contemporary Implant Dentistry* (2nd edition), Misch, C.E., (Ed.), 329-343, Mosby, ISBN 0815170599, St. Louis, MO

Misch, C.E., Bidez, M.W., Sharawy, M. (2001). A bioengineered implant for a predentermined bone cellular response to loading forces. *Journal of Periodontology*, Vol.72, No.9, (Sep 2001), pp. 1276-86

Morris, H.F., Winkler, S., Ochi, S., Kanaan, A. (2001). A new implant designed to maximize contact with trabecular bone: Survival to 18 months. *Journal of Oral Implantology*, Vol.27, No.4, pp. 164-173

Moscovitch, M. (2001). Molar restorations supported by 2 implants: An alternative to wide implants. J *can Dent assoc*, Vol.67, pp. 535-539

Moser, W. Nentwig, G.H. (1989). Finite Element Studien zur Optimierung von Implantat-gewindeformen. *Z Zhanarztl Implantol*, Vol.5, pp. 29-32

Munir, Z.A., Richards, L.W., Prado, M.E. (1975). Photoelastic studies of the stress distributions on blade-type endosteal dental implants. *J. Oral Implantol.*, Vol.5, No.3, pp. 296-332

Papavasiliou, G., Kamposiora, P., Bayne S.C., Felton D.A. (1996a). Three-dimensional finite element analysis of stress distribution around single tooth implants as a function of bony support, prosthesis type, and loading during function. *The Journal of Prosthetic Dentistry*, Vol.76, No.6, pp. 633-40

Papavasiliou, G., Tripodakis, A.P., Kamposiora, P., Strub, J.R., Bayne S.C. (1996b). Finite element analysis of ceramic abutment-restoration combinations for osseointegrated implants. *The International Journal of Prosthodontics*, Vol.9, No.3, (May-Jun 1996), pp. 254-60

Patra, A.K., DePaolo, J.M., D'Souza, K.S., DeTolla, D., Meenaghan, M.A. (1998). Guidelines for analysis and redesign of dental implants. *Implant Dentistry*, Vol.7, No.4, pp. 355-68

Pérez, M.A., Fornells, P., Doblaré, M. & García-Aznar, J.M. (2010). Comparative analysis of bone remdelling models with respect to computerised tomography-based finite element models of bone. Computer Methods in Biomechanics and Biomedical Engineering, Vol. 13, No. 1, (February 2010), pp. 71-80, ISSN 1476-8259

Pierrisnard, L., Hure, G., Barquins, M., Chappard, D. (2002). Two dental implants designed for immediate loading: a finite element analysis. *Int J Oral Maxillofac Implants*, Vol.17, No.3, pp. 353-362

Renouard, F., Arnous, J.P., Sarment, D.P. (1999). Five-mm-diameter implants without a smooth surface collar: Report on 98 consecutive placements. *Int J Oral Maxillofac Implants*. Vol 14:101-107

Rieger, M.R. (1988). Finite element stress analysis of root-form implants. *The Journal Of Oral Implantology*, Vol.14, No.4, pp. 472-84

Rieger, M.R., Fareed, K., Adams, W.K., Tanquist, R.A. (1989a). Bone stress distribution for three endosseous implants. *The Journal of Prosthetic Dentistry*, Vol.61, No.2, (Feb 1989), pp. 223-8

Rieger, M.R., Adams, W.K., Kinzel, G.L., Brose, M.O. (1989b). Finite element analysis of bone-adapted and bone-bonded endosseous implants, *J. Prosth. Dent*, Vol.64, No.5, pp. 436-40

Rieger, M.R., Adams, W.K., Kinzel G.L. (1990a). A finite element survey of eleven endosseous implants. *The Journal Of Prosthetic Dentistry*, Vol.63, No.4, pp. 457-65

Rieger, M.R., Mayberry, M., Brose, M.O. (1990b). Finite element analysis of six endosseous implants. *The Journal of Prosthetic Dentistry*, Vol.63, No.6, pp. 671-6

Reina, J.M., García-Aznar, J.M., Dominguez, J. & Doblaré, M. (2007). Numerical estimation of bone density and elastic constants distribution in a human mandible. *Journal of Biomechanics*, Vol. 40, No. 4, (May 2006), pp. 828-836, ISSN 0021-9290

Salama, H., Rose, L.F., Salama, M., Betts, N.J. (1995). Immediate loading of bilaterally splinted titanium root-form implants in fixed prosthodontics-a technique reexamined: two case reports. *The International Journal of Periodontics & Restorative Dentistry*, Vol.15, No.4, (August 1995), pp. 344-61

Sato, Y., Shindoi, N., Hosokawa, R., Tsuga, K., Akagawa, Y. (2000). Biomechanical effects of double or wide implants for single molar replacement in the posterior mandibular region. *Journal of Oral Rehabilitation*, Vol.27, No.10, pp. 842-5

Schenk, R.K. & Buser, D. (1998). Osseointegration: a reality. *Periodontology 2000*, Vol. 17, (Jun 1988), pp. 22-35, ISSN 1600-0757

Siegele, D., Soltesz, U. (1989). Numerical investigations of the influence of implant shape on stress distribution in the jaw bone. *The International Journal Of Oral & Maxillofacial Implants*, Vol.4, No.4, (Winter 1989), pp. 333-40

Simmons, C.A., Meguid, S.A. & Pilliar, R.M. (2001). Differences in osseointegration rate due to implant surface geometry can be explained by local tissue strains. *Journal of Orthopaedic Research*, Vol. 19, No. 2, (March 2001), pp. 187-194, ISSN 1554-527X

Skalak, R. (1988). Stress transfer at the implant interface. *J Oral Implantol*. Vol.13, pp. 531-593

Stegaroiu, R., Kusakari, H., Nishiyama, S., Miyakawa, O. (1998a). Influence of prosthesis material on stress distribution in bone and implant: a 3-dimensional finite element analysis. *The International Journal of Oral & Maxillofacial Implants*, Vol.13, No.6, (Nov-Dec 1998), pp. 781-90

Stegaroiu, R., Sato, T., Kusakari, H., Miyakawa, O. (1998b). Influence of restoration type on stress distribution in bone around implants: a three-dimensional finite element analysis. *The International Journal of Oral & Maxillofacial Implants*, Vol.13, No.1, (Jan-Feb 1998), pp. 82-90

Steinemann, S. (1996). The properties of titanium, In: *Oral implantology. Basics. ITI Dental Implant system.* A. Schroeder, F. Sutter, D. Biser, G. Drekeler, (Ed.) 37-59, Thieme Medical Publishers, New York

Tarnow, D.P., Emtiaz, S., Classi, A. (1997). Immediate loading of threaded implants at stage 1 surgery in edentulous arches: ten consecutive case reports with 1- to 5- year data.

The International Journal of Oral & Maxillofacial Implants, Vol.12, No.3, (May-June 1997), pp. 319-24

Trauhlar, R.S., Farish, S.E., Scheitler,L.E., Morris, H.F., Ochi, S. (1997). Bone quality and implant design-related outcomes through stage II surgical uncovering of spectra-system root form implants. *J Oral Maxillofac Surg*. Vp;/ 55, pp. 46-54

Tuncelli, B., Poyrazoglu, E., Köylüoglu, A.M., Tezcan, S. (1997). Comparison of load transfer by angulated, standard and inclined implant abutments. *The European Journal Of Prosthodontics And Restorative Dentistry*, Vol.5, No.2, (Jun 1997), pp. 85-8

Vaillancourt, H., Pilliar, R.M., McCammond, D. (1995). Finite element analysis of crestal bone loss around porous coated dental implants. *Journal of Applied Biomaterials*. Vol.6, No.4, pp. 267-282

Van Oosterwyck, H., Duyck, J., Vander Sloten, J., Van Der Perre, G., Naert, I. (2002). Peri-implant bone tissue strains in cases of dehiscence: a finite element study. *Clin oral Implants Res 2002*, Vol.13, No.3, pp. 327-333

Watzak, G., Zechner, W., Ulm, C., Tangl, S., Tepper, G. & Watzek, G. (2005). Histologic and histomorphometric analysis of three types of dental implants following 18 months of occlusal loading: a preliminary study in baboons. *Clinical Oral Implants Research*, Vol. 16, No. 4, (August 2005), pp. 408-416, ISSN 1600-0501

Weinans, H., Huiskes, R., & Grootenboer, H.J. (1992). Effects of material properties of femoral hip components on bone remodeling, *Journal of Orthopaedic Research*, Vol. 10, No. 6, (November 1992), pp. 845-853, ISSN 1554-527X

Weinans, H., Huiskes, R., van Rietbergen, B., Sumner, D.R., Turner, T.M. & Galante, J.O. (1993). Adaptive bone remodeling around bonded noncemented total hip arthroplasty: a comparison between animal experiments and computer simulation. *Journal of Orthopaedic Research*, Vol. 11, No. 4, (July 1993), pp. 500-513, ISSN 1554-527X

Weinstein A.M., Klawitter J.J., Anand S.C., Schuessler R. (1976). Stress analysis of porous rooted dental implants. *Journal Of Dental Research*, Vol.55, No.5, (Sep-Oct 1976), pp. 772-7

Wolff, J. (1892). *Das Gesetz der Transformation der Knochen*, Hirschwald, Berlin

Wolff, J. (1986). *The Law of Bone Remodelling*, Springer, ISBN 354016281X, Berlin

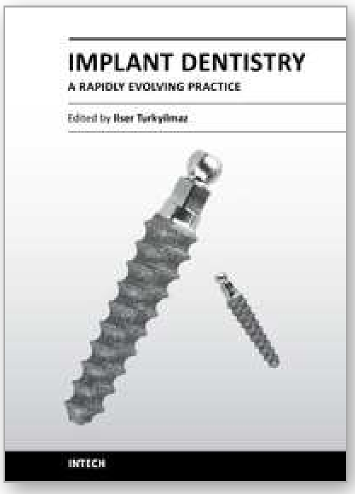

Implant Dentistry - A Rapidly Evolving Practice

Edited by Prof. Ilser Turkyilmaz

ISBN 978-953-307-658-4
Hard cover, 544 pages
Publisher InTech
Published online 29, August, 2011
Published in print edition August, 2011

Implant dentistry has come a long way since Dr. Branemark introduced the osseointegration concept with endosseous implants. The use of dental implants has increased exponentially in the last three decades. As implant treatment became more predictable, the benefits of therapy became evident. The demand for dental implants has fueled a rapid expansion of the market. Presently, general dentists and a variety of specialists offer implants as a solution to partial and complete edentulism. Implant dentistry continues to evolve and expand with the development of new surgical and prosthodontic techniques. The aim of Implant Dentistry - A Rapidly Evolving Practice, is to provide a comtemporary clinic resource for dentists who want to replace missing teeth with dental implants. It is a text that relates one chapter to every other chapter and integrates common threads among science, clinical experience and future concepts. This book consists of 23 chapters divided into five sections. We believe that, Implant Dentistry: A Rapidly Evolving Practice, will be a valuable source for dental students, post-graduate residents, general dentists and specialists who want to know more about dental implants.

InTech Europe
University Campus STeP Ri
Slavka Krautzeka 83/A
51000 Rijeka, Croatia
Phone: +385 (51) 770 447
Fax: +385 (51) 686 166
www.intechopen.com

InTech China
Unit 405, Office Block, Hotel Equatorial Shanghai
No.65, Yan An Road (West), Shanghai, 200040, China
中国上海市延安西路65号上海国际贵都大饭店办公楼405单元
Phone: +86-21-62489820
Fax: +86-21-62489821